Journal of Computational and Applied Mathematics 465 (2025) 116592

Contents lists available at ScienceDirect

Journal of Computational and Applied Mathematics

journal homepage: www.elsevier.com/locate/cam

Algebraic characterization of planar cubic and quintic Pythagorean-Hodograph B-spline curves

Lucia Romani [a], Alberto Viscardi [b,*]

[a] Dipartimento di Matematica, Alma Mater Studiorum Università di Bologna, Piazza di Porta San Donato 5, 40126 Bologna, Italy
[b] Dipartimento di Matematica "Giuseppe Peano", Università di Torino, Via Carlo Alberto 10, 10123 Torino, Italy

ARTICLE INFO

Keywords:
Planar curve
Non-uniform B-splines
Pythagorean-Hodograph
Control-polygon constraints
Complex representation

ABSTRACT

We provide a revised representation of planar cubic and quintic Pythagorean-Hodograph B-spline curves (PH B-splines for short) that offers the following advantages: (i) the clamped and closed cases are mostly treated together; (ii) the closed case is represented by using the minimum possible number of knots thus avoiding useless control points as well as control edges of zero length when the curve is regular. The proposed simplified representation turns out to be extremely useful to provide a unified *complex* algebraic characterization of clamped and closed planar PH B-splines of degree three and five. This is aimed at distinguishing regular planar cubic and quintic PH B-splines from C^1 cubic and C^2 quintic B-spline curves in general. As for planar cubic PH B-splines consisting of m pieces, we obtain m complex conditions that, differently from what was known so far, can be used to characterize both the clamped and the closed case. As for planar quintic PH B-splines, the complex conditions are $2m$ and, unlike what is shown for cubic PH B-splines, they also depend on the knot intervals. This is to be considered a completely new result since no *complex* algebraic characterization working for any arbitrarily chosen knot partition had ever been provided for either clamped or closed planar quintic PH B-splines. The proposed algebraic characterization is finally exploited to fully identify the preimage of a regular planar quintic PH B-spline resolving all the sign ambiguities that affected the existing results.

1. Introduction

Pythagorean-Hodograph B-spline curves (also known as PH B-splines) are a generalization of Pythagorean-Hodograph (PH) Bézier curves [1,2]. Indeed, PH B-splines are piecewise-polynomial parametric curves for which the Euclidean norm of the hodograph, that is its first derivative with respect to the parameter, is a polynomial B-spline. For a planar Pythagorean-Hodograph B-spline curve this means that the two derivative components and the parametric speed form a Pythagorean triple, whereas for a spatial Pythagorean-Hodograph B-spline curve the three derivative components and the parametric speed form a Pythagorean quadruple.

Several recent works focused on PH B-splines, using them either to solve interpolation problems of various kinds (see, e.g., [3–6]) or to build new extensions [7,8]. In the first group of the above mentioned papers, special attention is devoted to low-degree PH B-splines (in particular to the cubic and quintic ones). However, so far, no one has ever introduced for such curves, considered in their most general representation, a rigorous algebraic characterization in complex form. In particular, to the best of our knowledge, the first paper that started to deal with planar C^2 quintic PH splines (namely [9]) neither provides the minimal B-spline representation of non-uniformly parametrized curves of that kind, nor offers an algebraic characterization that allows users to easily

* Corresponding author.
E-mail addresses: lucia.romani@unibo.it (L. Romani), alberto.viscardi@unito.it (A. Viscardi).

https://doi.org/10.1016/j.cam.2025.116592
Received 29 July 2024; Received in revised form 15 January 2025
Available online 23 February 2025

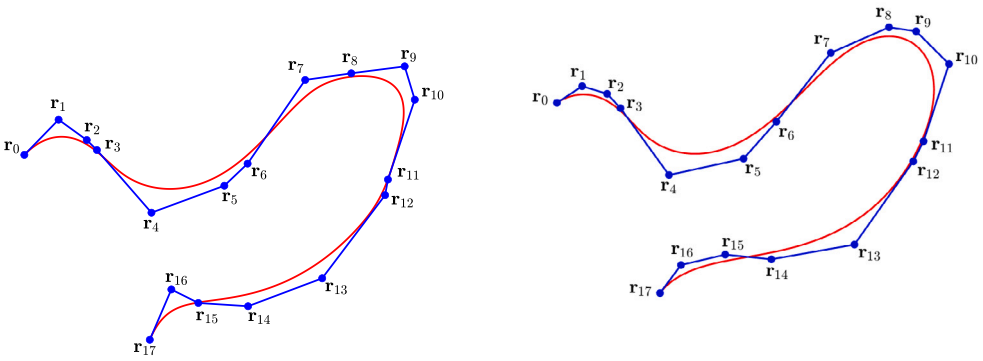

Fig. 1. Examples of C^2 B-spline curves sharing the same degree (five) and the same knot partition. Left: a C^2 quintic B-spline curve which is not a PH. Right: a C^2 quintic PH B-spline curve.

and straightforwardly establish whether the spline representation satisfies the PH property or not. Thus, our goal is to provide a simple tool to verify if a given C^2 quintic spline is a PH or not (see Fig. 1). As highlighted in [9], until now the problem had been solved, at a higher price, by using knot insertion to isolate all spline segments as single Bézier curves and, after reparametrizing each over $[0,1]$, testing all of them one at a time. Without knowing the conditions to be applied on the spline representation, this was certainly the only possible way to do it having only the conditions for the Bézier quintic case available. In particular, to distinguish quintic PH curves from general quintic Bézier curves it was possible to rely either on the real conditions in [10] or on their complex counterparts published in [11], [12, page 415] and successively improved in [13]. In this paper we show that it is not necessary to go through the conversion into Bézier pieces since one can check the PH property directly on the spline curve. In particular, for quintic spline curves consisting of m pieces, the check is encapsulated in $2m$ *complex* algebraic conditions. Differently from the cubic case where the conditions are only m and independent of the knot partition, in the quintic case the knot intervals do affect the algebraic conditions. This result is obtained after carefully revising the original representation of closed PH B-splines so that the minimum possible number of knots is used and useless control points are avoided.

More precisely, the remainder of the paper is organized as follows. In Section 2 we start by settling the notation and recalling some basic definitions and results. Then in Sections 3 and 4 we provide a unified representation of clamped and closed planar PH B-spline curves of degree three and five, respectively, along with conditions on their preimage in order to have closed ones. The proposed representation, in addition to being cheaper than the one introduced in [1] for the closed case, allows us to avoid also control edges of zero length when the curve is regular. Moreover, it allows us to obtain straightforwardly a unified algebraic characterization of clamped and closed PH B-splines of degree three (Section 3.1). The derivation of the algebraic characterization of quintic PH B-splines, instead, is more challenging and requires some computations that we collect in Section 4.1. For both cubic and quintic degrees the benefits brought by the introduced algebraic characterization in terms of preimage identification are highlighted. Conclusions and future lines of research are drawn in Section 5.

2. Preliminaries

Definition 1. Let $g, m \in \mathbb{N}$. Denoting with $\langle t \rangle^k$ the knot $t \in \mathbb{R}$ taken with multiplicity $k \in \mathbb{N}$, consider an (ordered) knot sequence in $\mathbb{R}$ of the form

$$\boldsymbol{\rho} \;=\; \{\, \langle t_{1-L} \rangle^{k_{1-L}} \;\leq\; \dots \;\leq\; \langle a \equiv t_1 \rangle^{k_1} \;<\; \dots \;<\; \langle t_{m+1} \equiv b \rangle^{k_{m+1}} \;\leq\; \dots \;\leq\; \langle t_{m+1+R} \rangle^{k_{m+1+R}} \,\},$$

for some $L, R \in \{0, \dots, g\}$ and $k_j \in \{1, \dots, g+1\}$, $j \in \{1-L, \dots, m+1+R\}$, with

$$\sum_{j=-L}^{0} k_{1+j} \;=\; \sum_{j=0}^{R} k_{m+1+j} \;=\; g+1.$$

A degree-g planar (complex) B-spline curve consisting of m polynomial pieces over the knot partition $\boldsymbol{\rho}$ is a function $\mathbf{r} : [a,b] \to \mathbb{C}$ of the form

$$\mathbf{r}(t) = \sum_{i=0}^{M+g} \mathbf{r}_i \, N^g_{i,\boldsymbol{\rho}}(t),$$

where

$$M \;=\; \sum_{j=2}^{m} k_j$$

is the sum of the multiplicities of all knots of $\boldsymbol{\rho}$ in $]a,b[$, $\{\mathbf{r}_i \in \mathbb{C}\}_{i=0}^{M+g}$ are the so called control points of the curve and $\{N^g_{i,\boldsymbol{\rho}}(t)\}_{i=0}^{M+g}$ are the degree-g B-spline basis functions over $\boldsymbol{\rho}$.

The hodograph of $\mathbf{r}(t)$, denoted with $\mathbf{p}(t)$, is the planar B-spline curve of degree $g-1$ defined over the knot partition

$$\boldsymbol{\nu} = \{ \langle t_{1-L}\rangle^{k_{1-L}-1} \le \dots \le \langle a \equiv t_1\rangle^{k_1} < \dots < \langle t_{m+1} \equiv b\rangle^{k_{m+1}} \le \dots \le \langle t_{m+1+R}\rangle^{k_{m+1+R}-1} \}$$

(here t_{1-L} and t_{m+1+R} are not considered if $k_{1-L}=1$ and $k_{m+1+R}=1$, respectively) with control points $\{\mathbf{p}_i \in \mathbb{C}\}_{i=0}^{M+g-1}$, i.e.,

$$\mathbf{p}(t) = \sum_{i=0}^{M+g-1} \mathbf{p}_i \, N_{i,\boldsymbol{\nu}}^{g-1}(t), \tag{1}$$

such that $\mathbf{r}'(t) = \mathbf{p}(t)$. Furthermore, $\mathbf{r}(t)$ is said to be regular if $\mathbf{p}(t) \neq \mathbf{0}$ for every $t \in [a,b]$.

A regular planar B-spline $\mathbf{r}(t)$ is said to be a Pythagorean Hodograph (PH) B-spline if its parametric speed $|\mathbf{p}(t)| \neq 0$ is a (real) B-spline.

It is well known [1] that, in order for $|\mathbf{p}(t)| \neq 0$ to be a (real) B-spline, there must exist a planar (complex) B-spline $\mathbf{z}(t)$ called *preimage* of $\mathbf{r}(t)$, such that, over $[a,b]$, $\mathbf{p}(t) = \mathbf{z}^2(t)$ and $\mathbf{z}(t) \neq 0$. This fact alone has many implications on the structure of $\mathbf{r}(t)$, $\mathbf{p}(t)$ and $\mathbf{z}(t)$. From (1), we have first that the degree of $\mathbf{p}(t)$ must be even and so the degree g of $\mathbf{r}(t)$ must be odd. Then, we need

$$\mathbf{z}(t) = \sum_{j=0}^{m+(g-1)/2-1} \mathbf{z}_j \, N_{j,\boldsymbol{\mu}}^{(g-1)/2}(t),$$

for some $\{\mathbf{z}_j \in \mathbb{C}\}_{j=0}^{m+(g-1)/2-1}$, where we choose

$$\boldsymbol{\mu} = \{ \langle t_0\rangle^{\frac{g-1}{2}} \le a \equiv t_1 < t_2 < \dots < t_m < t_{m+1} \equiv b \le \langle t_{m+2}\rangle^{\frac{g-1}{2}} \}. \tag{2}$$

The choice of (2) instead of the more general knot partition

$$\{ t_{1-(g-1)/2} \le \dots \le a \equiv t_1 < \dots < t_{m+1} \equiv b \le \dots \le t_{m+(g-1)/2+1} \},$$

is one of the key choices that allows us to treat the clamped and closed cases together. Since $\mathbf{p}(t)$ is obtained by squaring $\mathbf{z}(t)$, and $\mathbf{r}(t)$ is obtained by integrating $\mathbf{p}(t)$, we will be able to choose

$$\boldsymbol{\nu} = \{ \langle t_0\rangle^{\frac{g-1}{2}} \le \langle a \equiv t_1\rangle^{\frac{g+1}{2}} < \langle t_2\rangle^{\frac{g+1}{2}} < \dots < \langle t_m\rangle^{\frac{g+1}{2}} < \langle t_{m+1} \equiv b\rangle^{\frac{g+1}{2}} \le \langle t_{m+2}\rangle^{\frac{g-1}{2}} \}, \tag{3}$$

and thus

$$\boldsymbol{\rho} = \{ \langle t_0\rangle^{\frac{g+1}{2}} \le \langle a \equiv t_1\rangle^{\frac{g+1}{2}} < \langle t_2\rangle^{\frac{g+1}{2}} < \dots < \langle t_m\rangle^{\frac{g+1}{2}} < \langle t_{m+1} \equiv b\rangle^{\frac{g+1}{2}} \le \langle t_{m+2}\rangle^{\frac{g+1}{2}} \}. \tag{4}$$

In the following, when the specific cases $g \in \{3,5\}$ are investigated, we illustrate why the choices (2), (3) and (4) are feasible and good for our purposes. However, we emphasize right now that the arguments considered in our analysis can be easily extended to any degree $g \in 2\mathbb{N}-1$. We also point out that, for the sake of conciseness, from now on we will use the notation

$$d_j = t_{j+1} - t_j, \qquad j = 0, \dots, m+1, \tag{5}$$

to refer to the knot intervals identified by the knot partitions $\boldsymbol{\mu}$, $\boldsymbol{\nu}$, $\boldsymbol{\rho}$ in (2), (3), (4), respectively. We also highlight that $d_j > 0$ for $j \in \{1, \dots, m\}$ whereas $d_j \ge 0$ for $j \in \{0, m+1\}$.

3. Planar cubic PH B-splines

Specializing the definition introduced in Section 2 for the cubic case, i.e., $g=3$, we have that a planar cubic PH B-spline $\mathbf{r}(t)$ with $m \in \mathbb{N}$ pieces is defined by $2m+2$ control points $\{\mathbf{r}_i \in \mathbb{C}\}_{i=0}^{2m+1}$ over a knot partition of the form

$$\boldsymbol{\rho} = \{ \langle t_0\rangle^2 \le \langle a \equiv t_1\rangle^2 < \langle t_2\rangle^2 < \dots < \langle t_m\rangle^2 < \langle t_{m+1} \equiv b\rangle^2 \le \langle t_{m+2}\rangle^2 \},$$

so that

$$\mathbf{r}(t) = \sum_{i=0}^{2m+1} \mathbf{r}_i \, N_{i,\boldsymbol{\rho}}^3(t), \qquad t \in [a,b]. \tag{6}$$

The hodograph $\mathbf{p}(t)$ of the cubic PH B-spline $\mathbf{r}(t)$ is a quadratic B-spline defined by the control points $\{\mathbf{p}_i \in \mathbb{C}\}_{i=0}^{2m}$ over the knot partition

$$\boldsymbol{\nu} = \{ t_0 \le \langle a \equiv t_1\rangle^2 < \langle t_2\rangle^2 < \dots < \langle t_m\rangle^2 < \langle t_{m+1} \equiv b\rangle^2 \le t_{m+2} \},$$

satisfying

$$\mathbf{p}(t) = \sum_{i=0}^{2m} \mathbf{p}_i \, N_{i,\boldsymbol{\nu}}^2(t) = \mathbf{r}'(t) = \mathbf{z}^2(t), \qquad t \in [a,b], \tag{7}$$

where $\mathbf{z}(t)$ is its preimage, i.e., a linear B-spline defined by the control points $\{\mathbf{z}_j \in \mathbb{C}\}_{j=0}^{m}$ over the partition

$$\boldsymbol{\mu} = \{ t_0 \le a \equiv t_1 < t_2 < \dots < t_m < t_{m+1} \equiv b \le t_{m+2} \},$$

as

$$\mathbf{z}(t) \;=\; \sum_{j=0}^{m} \mathbf{z}_j \, N^1_{j,\boldsymbol{\mu}}(t), \qquad t \in [a,b].$$

Since $\mathbf{z}(t) \in C^0([a,b],\mathbb{C})$, $\mathbf{p}(t) = \mathbf{z}^2(t)$ and $\mathbf{r}'(t) = \mathbf{p}(t)$, we have that $\mathbf{p}(t) \in C^0([a,b],\mathbb{C})$ and $\mathbf{r}(t) \in C^1([a,b],\mathbb{C})$. Moreover, the following relations between the control points of $\mathbf{r}(t)$, $\mathbf{p}(t)$ and $\mathbf{z}(t)$ must hold (see [1]):

$$\begin{cases} \mathbf{r}_{2j} \;=\; \mathbf{r}_{2j-1} \;+\; \dfrac{d_j}{3}\,\mathbf{p}_{2j-1}, & j \in \{1,\dots,m\}, \\ \mathbf{r}_{2j+1} \;=\; \mathbf{r}_{2j} \;+\; \dfrac{d_j + d_{j+1}}{3}\,\mathbf{p}_{2j}, & j \in \{0,\dots,m\}, \end{cases} \tag{8}$$

and

$$\begin{cases} \mathbf{p}_{2j} \;=\; \mathbf{z}_j^2, & j \in \{0,\dots,m\}, \\ \mathbf{p}_{2j+1} \;=\; \mathbf{z}_j\,\mathbf{z}_{j+1}, & j \in \{0,\dots,m-1\}. \end{cases} \tag{9}$$

Remark 1. Following [14,15], it turns out that the correct knot partition for describing $\mathbf{z}^2(t)$ is

$$\widetilde{\boldsymbol{\nu}} \;=\; \{\; \langle t_0\rangle^2 \;\le\; \langle a \equiv t_1\rangle^2 \;<\; \langle t_2\rangle^2 \;<\; \dots \;<\; \langle t_m\rangle^2 \;<\; \langle t_{m+1} \equiv b\rangle^2 \;\le\; \langle t_{m+2}\rangle^2 \;\}.$$

Thus, in general, there might exist $\widetilde{t} \notin [a,b]$ such that $\mathbf{z}^2(\widetilde{t}) \neq \mathbf{p}(\widetilde{t})$, but this does not affect the results presented here since (9) guarantees $\mathbf{z}^2(t) = \mathbf{p}(t)$ for all $t \in [a,b]$. Indeed, going from $\widetilde{\boldsymbol{\nu}}$ to $\boldsymbol{\nu}$ we are only loosing two quadratic B-spline basis functions, namely the ones built over the knots $\{\langle t_0\rangle^2, \langle t_1\rangle^2\}$ and $\{\langle t_{m+1}\rangle^2, \langle t_{m+2}\rangle^2\}$, respectively, which are supported outside $[a,b]$.

Below we analyze how the boundary knots t_0 and t_{m+2} must be selected to give rise to either a clamped or a closed cubic PH B-spline curve. Moreover, in the closed case, we specify how to choose $\mathbf{z}_m$ and $\mathbf{z}_{m-1}$ so that a regular cubic PH B-spline curve is C^1 at the closure point.

Clamped case: In order for $\mathbf{r}$ to be *clamped* we need to select the boundary knots t_0 and t_{m+2} so that

$$t_0 = t_1 \qquad \text{and} \qquad t_{m+2} = t_{m+1},$$

which implies

$$d_0 = 0 \qquad \text{and} \qquad d_{m+1} = 0. \tag{10}$$

Closed case: In order for $\mathbf{r}$ to be *closed* we need to set $m \ge 2$ and select t_0 and t_{m+2} so that

$$t_0 = t_1 - (t_{m+1} - t_m) \qquad \text{and} \qquad t_{m+2} = t_{m+1} + (t_2 - t_1).$$

In particular, this implies

$$d_0 = d_m \qquad \text{and} \qquad d_{m+1} = d_1. \tag{11}$$

Moreover, in order for $\mathbf{r}$ to be such that $\mathbf{r}(a) = \mathbf{r}(b)$ and $\mathbf{r}'(a) = \mathbf{r}'(b)$ (so that C^1 continuity holds at the closure point whenever $\mathbf{r}$ is regular), we also need to require the constraints (see [1, Eq. (18)])

$$\sum_{i=0}^{2m-1} D_i\,\mathbf{p}_i \;=\; 0 \qquad \text{and} \qquad \sum_{i=1}^{2m} D_i\,\mathbf{p}_i \;=\; 0 \tag{12}$$

where

$$\begin{cases} D_{2j} \;=\; d_j + d_{j+1}, & j \in \{0,\dots,m\}, \\ D_{2j+1} \;=\; d_{j+1}, & j \in \{0,\dots,m-1\}. \end{cases}$$

Conditions (12) are fulfilled by setting

$$\mathbf{z}_m = \pm\,\mathbf{z}_0 \qquad \text{and} \qquad \mathbf{z}_{m-1} = \frac{-\boldsymbol{\beta}_1 \;\pm\; \sqrt{\boldsymbol{\beta}_1^2 - 4\,\alpha_1\,\boldsymbol{\gamma}_1}}{2\alpha_1}, \tag{13}$$

with

$$\begin{aligned} \alpha_1 &= d_{m-1} + d_m, \\ \boldsymbol{\beta}_1 &= d_{m-1}\,\mathbf{z}_{m-2} + d_m\,\mathbf{z}_m, \\ \boldsymbol{\gamma}_1 &= \sum_{j=1}^{m-1} (d_{j-1} + d_j)\,\mathbf{z}_{j-1}^2 + \sum_{j=1}^{m-2} d_j\,\mathbf{z}_{j-1}\mathbf{z}_j. \end{aligned}$$

Since, in view of (8),

$$\mathbf{r}_{2m} = \mathbf{r}_0 + \sum_{i=0}^{2m-1} \frac{D_i}{3}\,\mathbf{p}_i \qquad \text{and} \qquad \mathbf{r}_{2m+1} = \mathbf{r}_1 + \sum_{i=1}^{2m} \frac{D_i}{3}\,\mathbf{p}_i,$$

we emphasize that conditions (12) imply

$$\mathbf{r}_{2m} = \mathbf{r}_0 \qquad \text{and} \qquad \mathbf{r}_{2m+1} = \mathbf{r}_1. \tag{14}$$

Additionally, in view of (11) and (12), it also turns out that the last and the first control point of $\mathbf{p}$ satisfy

$$\mathbf{p}_{2m} = \mathbf{p}_0.$$

When $m = 2$ and $\mathbf{z}_2 = -\mathbf{z}_0$, using (9) it is easy to prove that

$$\frac{\mathbf{p}_0}{\mathbf{z}_0\mathbf{z}_1} = \overline{\left(\frac{\mathbf{p}_2}{\mathbf{z}_0\mathbf{z}_1}\right)}, \qquad \frac{\mathbf{p}_1}{\mathbf{z}_0\mathbf{z}_1} = 1 \qquad \text{and} \qquad \frac{\mathbf{p}_3}{\mathbf{z}_0\mathbf{z}_1} = -1. \tag{15}$$

Thus, the control polygon $\{\mathbf{p}_0, \mathbf{p}_1, \mathbf{p}_2, \mathbf{p}_3\}$ is symmetric with respect to the line passing through $\mathbf{p}_1$ and $\mathbf{p}_3$. Similarly, using (8) and (11),

$$\frac{\mathbf{r}_1 - \mathbf{r}_0}{\mathbf{z}_0\mathbf{z}_1} = \frac{d_1 + d_2}{3}\frac{\mathbf{p}_0}{\mathbf{z}_0\mathbf{z}_1} = \frac{d_1 + d_2}{3}\overline{\left(\frac{\mathbf{p}_2}{\mathbf{z}_0\mathbf{z}_1}\right)} = \overline{\left(\frac{\mathbf{r}_3 - \mathbf{r}_2}{\mathbf{z}_0\mathbf{z}_1}\right)},$$
$$\frac{\mathbf{r}_2 - \mathbf{r}_1}{\mathbf{z}_0\mathbf{z}_1} = \frac{d_1}{3}\frac{\mathbf{p}_1}{\mathbf{z}_0\mathbf{z}_1} = \frac{d_1}{3} \qquad \text{and} \qquad \frac{\mathbf{r}_0 - \mathbf{r}_3}{\mathbf{z}_0\mathbf{z}_1} = \frac{\mathbf{r}_4 - \mathbf{r}_3}{\mathbf{z}_0\mathbf{z}_1} = \frac{d_2}{3}\frac{\mathbf{p}_3}{\mathbf{z}_0\mathbf{z}_1} = -\frac{d_2}{3}.$$

As a consequence, the control polygon $\{\mathbf{r}_0, \mathbf{r}_1, \mathbf{r}_2, \mathbf{r}_3\}$ is symmetric with respect to the line connecting $(\mathbf{r}_0+\mathbf{r}_3)/2$ and $(\mathbf{r}_1+\mathbf{r}_2)/2$.

Remark 2. We point out that, in the closed case, the new definition of $\mathbf{r}$ and $\mathbf{p}$ is the one that guarantees the minimum possible number of knots. Indeed, according to [15], the knot partition $\boldsymbol{\nu}$ associated to $\mathbf{p}(t) = \mathbf{z}^2(t)$ should be

$$\{\ \langle t_0\rangle^2 \ < \ \langle a \equiv t_1\rangle^2 \ < \ \langle t_2\rangle^2 \ < \ \dots \ < \ \langle t_m\rangle^2 \ < \ \langle t_{m+1} \equiv b\rangle^2 \ < \ \langle t_{m+2}\rangle^2 \ \}$$

but, in practice, the multiplicity of t_0 and t_{m+2} can be lowered by one since the support of the quadratic B-spline basis function that takes off from the first of the t_0s as well as the support of the quadratic B-spline basis function that ends at the last of the t_{m+2}s would not affect the domain $[a, b]$ and thus would have no influence on the definition of $\mathbf{p}$. Hence, differently from [1], Eq. (6) for a closed cubic PH spline with m polynomial pieces has two fewer control points, i.e., $2m + 2$ control points rather than $2m + 4$ as suggested in [1] (see, e.g., Figs. 2 and 3 and compare (6) with [1, page 70]).

3.1. The unified complex algebraic characterization

Thanks to the newly proposed unified formulation of clamped and closed cubic PH B-splines, we can reach a unified complex algebraic characterization of such curves which encompasses the following m conditions

$$\mathbf{p}_{2j+1}^2 = \mathbf{p}_{2j}\,\mathbf{p}_{2j+2}, \qquad j \in \{0, \dots, m-1\}. \tag{16}$$

This is a natural consequence of (9) and, as expected, the number of constraints to be satisfied by the control edges of a C^1 cubic B-spline curve to identify a PH cubic B-spline is one per spline segment. Moreover, in the clamped case with $m = 1$, (16) gives us back the well-known algebraic characterization of cubic PH Bézier curves [11]. Indeed, from (8), it follows that the relationship between the control edges $\{\mathbf{e}_i = \mathbf{r}_{i+1} - \mathbf{r}_i\}_{i=0}^{2m}$ of $\mathbf{r}(t)$ and the hodograph control points $\{\mathbf{p}_i\}_{i=0}^{2m}$ is

$$\begin{cases} \mathbf{e}_{2j} = \mathbf{r}_{2j+1} - \mathbf{r}_{2j} = \dfrac{d_j + d_{j+1}}{3}\mathbf{p}_{2j} = \dfrac{D_{2j}}{3}\mathbf{p}_{2j}, & j \in \{0, \dots, m\}, \\ \mathbf{e}_{2j+1} = \mathbf{r}_{2j+2} - \mathbf{r}_{2j+1} = \dfrac{d_{j+1}}{3}\mathbf{p}_{2j+1} = \dfrac{D_{2j+1}}{3}\mathbf{p}_{2j+1}, & j \in \{0, \dots, m-1\}. \end{cases}$$

As a consequence, (16) can be also rewritten as

$$\frac{\mathbf{e}_{2j+1}^2}{D_{2j+1}^2} = \frac{\mathbf{e}_{2j}\,\mathbf{e}_{2j+2}}{D_{2j}\,D_{2j+2}}, \qquad j \in \{0, \dots, m-1\}.$$

Therefore, recalling that, when $m = 1$ and the knot partition is clamped (i.e., (10) holds true),

$$D_0 = d_0 + d_1 = d_1, \qquad D_1 = d_1 \qquad \text{and} \qquad D_2 = d_1 + d_2 = d_1,$$

the well-known result $\mathbf{e}_1^2 = \mathbf{e}_0\mathbf{e}_2$ is then recovered straightforwardly. Instead, when the curve is closed, $m = 2$ and $\mathbf{z}_2 = -\mathbf{z}_0$, we observe that conditions (16), together with (15), lead to

$$\left|\frac{\mathbf{p}_0}{\mathbf{z}_0\mathbf{z}_1}\right| = \left|\frac{\mathbf{p}_2}{\mathbf{z}_0\mathbf{z}_1}\right| = 1.$$

The characterization given by conditions (16) allows us to verify if a given planar cubic B-spline is a PH B-spline using only the control points of the hodograph $\{\mathbf{p}_i\}_{i=0}^{2m}$. Conversely, given the control points of the hodograph satisfying (16), we are able to determine via (8) a regular planar cubic PH B-spline $\mathbf{r}(t)$ (unique up to a translation) and, of course, its parametric speed $|\mathbf{p}(t)|$. To close the circle, we conclude by proving that conditions (16) are enough also to identify the preimage $\mathbf{z}(t)$.

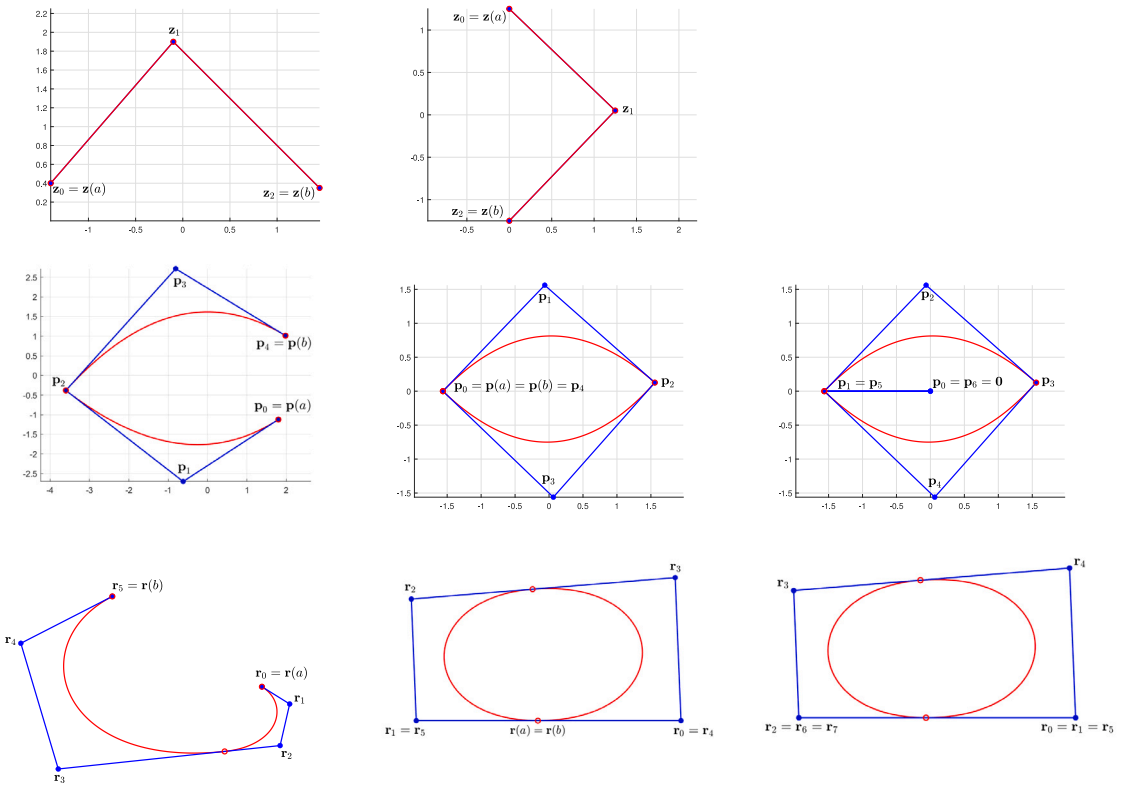

Fig. 2. Examples of cubic C^1 PH B-spline curves $\mathbf{r}(t)$ (third row), their quadratic C^0 hodographs $\mathbf{p}(t)$ (second row) and their linear C^0 preimages $\mathbf{z}(t)$ (first row). First column: clamped case with $m = 2$. Second column: closed case with $m = 2$. Third column: representation of $\mathbf{p}$ and $\mathbf{r}$ used in [1] to get the same B-spline curves in the second column. In all figures red circles emphasize the junction points between consecutive polynomial pieces.

Proposition 1. *Let* $\{\mathbf{p}_i \in \mathbb{C}\}_{i=0}^{2m}$ *satisfy* (16) *and let* $\mathbf{r}(t)$ *be the regular planar cubic PH B-spline with hodograph control points* $\{\mathbf{p}_i \in \mathbb{C}\}_{i=0}^{2m}$. *Then, for* $\mathbf{s} \in \{\pm\sqrt{\mathbf{p}_0}\}$, *the set of control points*

$$\mathbf{z}_0 \;=\; \mathbf{s} \qquad \textit{and} \qquad \mathbf{z}_j \;=\; \frac{\mathbf{p}_{2j-1}}{\mathbf{z}_{j-1}}, \qquad j \in \{1, \dots, m\}, \tag{17}$$

defines a preimage of $\mathbf{r}(t)$.

Proof. We start observing that, in order for $\mathbf{r}(t)$ to be regular, it must be $\mathbf{p}_i \neq 0$ for all $i \in \{0, \dots, 2m\}$. Indeed, due to (7), we have

$$0 \;\neq\; \mathbf{r}'(t_j) \;=\; \mathbf{p}_{2j-2}, \qquad j \in \{1, \dots, m+1\}.$$

Defining $\{\mathbf{z}_j \neq 0\}_{j=0}^{m}$ as in (17) leads to

$$\mathbf{z}_j\, \mathbf{z}_{j+1} \;=\; \mathbf{p}_{2j+1}, \qquad j \in \{0, \dots, m-1\}, \tag{18}$$

and, by (16),

$$\mathbf{z}_j^2\, \mathbf{z}_{j+1}^2 \;=\; \mathbf{p}_{2j+1}^2 \;=\; \mathbf{p}_{2j}\, \mathbf{p}_{2j+2}, \qquad j \in \{0, \dots, m-1\}.$$

Since $\mathbf{z}_0^2 = \mathbf{p}_0$, we then have

$$\mathbf{z}_j^2 \;=\; \mathbf{p}_{2j}, \qquad j \in \{1, \dots, m\}. \tag{19}$$

But (18) and (19) coincide with conditions (9) and so $\mathbf{r}'(t) = \mathbf{z}^2(t)$. □

Remark 3. For $\mathbf{s} \in \{\pm\sqrt{\mathbf{p}_0}\}$, we have that (17) can be equivalently written as

$$\mathbf{z}_j \;=\; \mathbf{s}^{(-1)^j} \prod_{k=1}^{j} \left(\mathbf{p}_{2k-1}\right)^{(-1)^{j-k}}, \qquad j \in \{0, \dots, m\}. \tag{20}$$

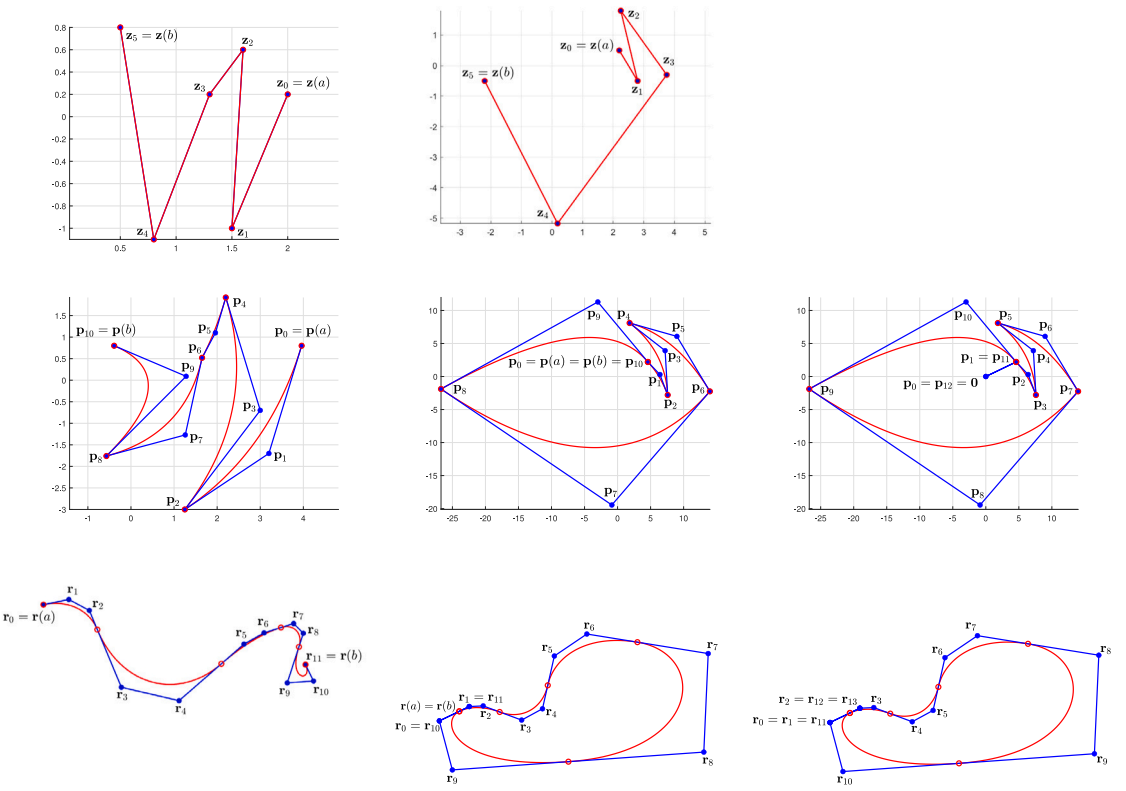

Fig. 3. Examples of cubic C^1 PH B-spline curves $\mathbf{r}(t)$ (third row), their quadratic C^0 hodographs $\mathbf{p}(t)$ (second row) and their linear C^0 preimages $\mathbf{z}(t)$ (first row). First column: clamped case with $m = 5$. Second column: closed case with $m = 5$. Third column: representation of $\mathbf{p}$ and $\mathbf{r}$ used in [1] to get the same B-spline curves in the second column. In all figures red circles emphasize the junction points between consecutive polynomial pieces.

Moreover, as expected by the relationship between $\mathbf{p}(t)$ and $\mathbf{z}(t)$, i.e. $\mathbf{p}(t) = \mathbf{z}^2(t)$, the preimage of $\mathbf{r}(t)$ is identified up to a sign, given by the choice of $\mathbf{s}$. With respect to the known result (see Eq. (40) and Eq. (42) in [1]), here (20) is without ambiguities about the signs of $\{\mathbf{z}_j\}_{j=0}^{m}$. This is a benefit brought by the algebraic characterization.

4. Planar quintic PH B-splines

Specializing the definition introduced in Section 2 for the quintic case, i.e., $g = 5$, we have that a planar quintic PH B-spline $\mathbf{r}(t)$ with $m \in \mathbb{N}$ pieces is defined by $3m+3$ control points $\{\mathbf{r}_i \in \mathbb{C}\}_{i=0}^{3m+2}$ over a knot partition

$$\boldsymbol{\rho} \;=\; \{\, \langle t_0\rangle^3 \;\le\; \langle a \equiv t_1\rangle^3 \;<\; \langle t_2\rangle^3 \;<\; \ldots \;<\; \langle t_m\rangle^3 \;<\; \langle t_{m+1} \equiv b\rangle^3 \;\le\; \langle t_{m+2}\rangle^3 \,\}, \tag{21}$$

so that

$$\mathbf{r}(t) \;=\; \sum_{i=0}^{3m+2} \mathbf{r}_i \, N^5_{i,\boldsymbol{\rho}}(t), \qquad t \in [a,b]. \tag{22}$$

The hodograph $\mathbf{p}(t)$ of the quintic PH B-spline $\mathbf{r}(t)$ is a quartic B-spline defined by the control points $\{\mathbf{p}_i \in \mathbb{C}\}_{i=0}^{3m+1}$ over the knot partition

$$\boldsymbol{\nu} \;=\; \{\, \langle t_0\rangle^2 \;\le\; \langle a \equiv t_1\rangle^3 \;<\; \langle t_2\rangle^3 \;<\; \ldots \;<\; \langle t_m\rangle^3 \;<\; \langle t_{m+1} \equiv b\rangle^3 \;\le\; \langle t_{m+2}\rangle^2 \,\},$$

satisfying

$$\mathbf{p}(t) \;=\; \sum_{i=0}^{3m+1} \mathbf{p}_i \, N^4_{i,\boldsymbol{\nu}}(t) \;=\; \mathbf{r}'(t) \;=\; \mathbf{z}^2(t), \qquad t \in [a,b], \tag{23}$$

where $\mathbf{z}(t)$ is its preimage, i.e., a quadratic B-spline defined by the control points $\{\mathbf{z}_j \in \mathbb{C}\}_{j=0}^{m+1}$ over the partition

$$\boldsymbol{\mu} \;=\; \{\, \langle t_0\rangle^2 \le\; a \equiv t_1 \;<\; t_2 \;<\; \ldots \;<\; t_m \;<\; t_{m+1} \equiv b \;\le\; \langle t_{m+2}\rangle^2 \,\}, \tag{24}$$

as

$$\mathbf{z}(t) \;=\; \sum_{j=0}^{m+1} \mathbf{z}_j \, N^2_{j,\boldsymbol{\mu}}(t), \qquad t \in [a,b]. \tag{25}$$

Since $\mathbf{z}(t) \in C^1([a,b],\mathbb{C})$, $\mathbf{p}(t) = \mathbf{z}^2(t)$ and $\mathbf{r}'(t) = \mathbf{p}(t)$, we have that $\mathbf{p}(t) \in C^1([a,b],\mathbb{C})$ and $\mathbf{r}(t) \in C^2([a,b],\mathbb{C})$. Moreover, the following relations between the control points of $\mathbf{r}(t)$, $\mathbf{p}(t)$ and $\mathbf{z}(t)$ must hold (see [1]):

$$\begin{cases} \mathbf{r}_{3j} \;=\; \mathbf{r}_{3j-1} \;+\; \dfrac{d_j}{5}\,\mathbf{p}_{3j-1}, & j \in \{1,\dots,m\}, \\ \mathbf{r}_{3j+1} \;=\; \mathbf{r}_{3j} \;+\; \dfrac{d_j + d_{j+1}}{5}\,\mathbf{p}_{3j}, & j \in \{0,\dots,m\}, \\ \mathbf{r}_{3j+2} \;=\; \mathbf{r}_{3j+1} \;+\; \dfrac{d_j + d_{j+1}}{5}\,\mathbf{p}_{3j+1}, & j \in \{0,\dots,m\}, \end{cases} \tag{26}$$

and

$$\begin{cases} \mathbf{p}_{3j} \;=\; \mathbf{z}_j \, \dfrac{d_{j+1}\mathbf{z}_j + d_j\mathbf{z}_{j+1}}{d_j + d_{j+1}}, & j \in \{0,\dots,m\}, \\ \mathbf{p}_{3j+1} \;=\; \mathbf{z}_{j+1} \, \dfrac{d_{j+1}\mathbf{z}_j + d_j\mathbf{z}_{j+1}}{d_j + d_{j+1}}, & j \in \{0,\dots,m\}, \\ \mathbf{p}_{3j+2} \;=\; \dfrac{2}{3}\mathbf{z}^2_{j+1} + \dfrac{1}{3}\left(\dfrac{d_{j+1}\mathbf{z}_j + d_j\mathbf{z}_{j+1}}{d_j + d_{j+1}}\right)\left(\dfrac{d_{j+2}\mathbf{z}_{j+1} + d_{j+1}\mathbf{z}_{j+2}}{d_{j+1} + d_{j+2}}\right), & j \in \{0,\dots,m-1\}. \end{cases} \tag{27}$$

Remark 4. Similarly to Remark 1, following [14,15], it turns out that the correct knot partition for describing $\mathbf{z}^2(t)$ is

$$\widetilde{\boldsymbol{\nu}} \;=\; \{\; \langle t_0\rangle^4 \;\le\; \langle a \equiv t_1\rangle^3 \;<\; \langle t_2\rangle^3 \;<\; \dots \;<\; \langle t_m\rangle^3 \;<\; \langle t_{m+1} \equiv b\rangle^3 \;\le\; \langle t_{m+2}\rangle^4 \;\}.$$

Thus, in general, there might exist $\widetilde{t} \notin [a,b]$ such that $\mathbf{z}^2(\widetilde{t}) \neq \mathbf{p}(\widetilde{t})$, but this does not affect the results presented here since (27) guarantees $\mathbf{z}^2(t) = \mathbf{p}(t)$ for all $t \in [a,b]$. Indeed, going from $\widetilde{\boldsymbol{\nu}}$ to $\boldsymbol{\nu}$ we are only loosing four quartic B-spline basis functions, namely the ones built over the knots $\{\langle t_0\rangle^4, \langle t_1\rangle^2\}$, $\{\langle t_0\rangle^3, \langle t_1\rangle^3\}$, $\{\langle t_{m+1}\rangle^3, \langle t_{m+2}\rangle^3\}$ and $\{\langle t_{m+1}\rangle^2, \langle t_{m+2}\rangle^4\}$, respectively, which are supported outside $[a,b]$.

Moreover, with respect to [1], here we are using the knot partition $\boldsymbol{\mu}$ in (24) for $\mathbf{z}(t)$ instead of

$$\widetilde{\boldsymbol{\mu}} \;=\; \{\; t_{-1} \;\le\; t_0 \;\le\; a \equiv t_1 \;<\; t_2 \;<\; \dots \;<\; t_m \;<\; t_{m+1} \equiv b \;\le\; t_{m+2} \;\le\; t_{m+3} \;\},$$

On the one hand, this allows us to unify the clamped and the closed cases, while, on the other hand, the definition of $\mathbf{z}$ over $[a,b]$ is not affected since, when restricted to the interval $[a,b]$, the quadratic B-spline basis functions over the knots $\{t_{-1}, t_0, t_1, t_2\}$ and $\{t_m, t_{m+1}, t_{m+2}, t_{m+3}\}$ of $\widetilde{\boldsymbol{\mu}}$ coincide respectively with the ones over the knots $\{\langle t_0\rangle^2, t_1, t_2\}$ and $\{t_m, t_{m+1}, \langle t_{m+2}\rangle^2\}$ of $\boldsymbol{\mu}$.

Below we point out how the boundary knots t_0 and t_{m+2} must be selected to give rise to either a clamped or a closed quintic PH B-spline curve. Moreover, in the closed case, we specify how to choose $\mathbf{z}_{m+1}$, $\mathbf{z}_m$ and $\mathbf{z}_{m-1}$ so that a regular quintic PH B-spline is C^2 at the closure point.

Clamped case: In order for $\mathbf{r}$ to be *clamped* we need to select the boundary knots t_0 and t_{m+2} so that

$$t_0 = t_1 \qquad \text{and} \qquad t_{m+2} = t_{m+1},$$

which implies

$$d_0 = 0 \qquad \text{and} \qquad d_{m+1} = 0. \tag{28}$$

Closed case: In order for $\mathbf{r}$ to be *closed* we need to set $m \ge 2$ and select t_0 and t_{m+2} so that

$$t_0 = t_1 - (t_{m+1} - t_m) \qquad \text{and} \qquad t_{m+2} = t_{m+1} + (t_2 - t_1).$$

The last conditions imply

$$d_0 = d_m \qquad \text{and} \qquad d_{m+1} = d_1. \tag{29}$$

Moreover, in order for $\mathbf{r}$ to be such that $\mathbf{r}(a) = \mathbf{r}(b)$, $\mathbf{r}'(a) = \mathbf{r}'(b)$, $\mathbf{r}''(a) = \mathbf{r}''(b)$ (so that C^2 continuity holds at the closure point whenever $\mathbf{r}$ is regular), we require the following constraints (see [1, Eq. (18)])

$$\sum_{i=2}^{3m+1} D_i\,\mathbf{p}_i = 0, \qquad \sum_{i=1}^{3m} D_i\,\mathbf{p}_i = 0 \qquad \text{and} \qquad \sum_{i=0}^{3m-1} D_i\,\mathbf{p}_i = 0, \tag{30}$$

where

$$\begin{cases} D_{3j} \;=\; d_j + d_{j+1}, & j \in \{0,\dots,m\}, \\ D_{3j+1} \;=\; d_j + d_{j+1}, & j \in \{0,\dots,m\}, \\ D_{3j+2} \;=\; d_{j+1}, & j \in \{0,\dots,m-1\}. \end{cases}$$

If $m > 2$ conditions (30) are fulfilled by setting

$$[\mathbf{z}_m, \mathbf{z}_{m+1}] = \pm\,[\mathbf{z}_0, \mathbf{z}_1] \qquad \text{and} \qquad \mathbf{z}_{m-1} = \frac{-\beta_2 \pm \sqrt{\beta_2^2 - 4\alpha_2\,\gamma_2}}{2\alpha_2},$$

with

$$\begin{aligned}
\alpha_2 &= d_{m-2} + \tfrac{2}{3}d_{m-1} + d_m + \tfrac{1}{3}\,\frac{d_{m-2}\,d_{m-1}\,d_m}{(d_{m-2}+d_{m-1})(d_{m-1}+d_m)}\,,\\
\beta_2 &= (d_{m-2}+d_{m-1})\,\mathbf{z}_{m-2} + (d_{m-1}+d_m)\,\mathbf{z}_m + \tfrac{1}{3}\,\frac{d_{m-2}^2\,(d_{m-2}\mathbf{z}_{m-3}+d_{m-3}\mathbf{z}_{m-2})}{(d_{m-3}+d_{m-2})(d_{m-2}+d_{m-1})}\\
&\quad + \tfrac{1}{3}\,\frac{d_{m-1}^2\,(d_m\mathbf{z}_{m-2}+d_{m-2}\mathbf{z}_m)}{(d_{m-2}+d_{m-1})(d_{m-1}+d_m)} + \tfrac{1}{3}\,\frac{d_m^2\,(d_{m+1}\mathbf{z}_m+d_m\mathbf{z}_{m+1})}{(d_{m-1}+d_m)(d_m+d_{m+1})}\,,\\
\gamma_2 &= \left(d_{m-1}+\tfrac{2}{3}d_{m-2}\right)\mathbf{z}_{m-2}^2 + \left(d_{m-1}+\tfrac{2}{3}d_m\right)\mathbf{z}_m^2 + \tfrac{1}{3}\,\frac{d_{m-1}^3\,\mathbf{z}_{m-2}\,\mathbf{z}_m}{(d_{m-2}+d_{m-1})(d_{m-1}+d_m)}\\
&\quad + \tfrac{1}{3}\,\frac{d_{m-2}\,d_{m-1}\,\mathbf{z}_{m-2}\,(d_{m-2}\mathbf{z}_{m-3}+d_{m-3}\mathbf{z}_{m-2})}{(d_{m-3}+d_{m-2})(d_{m-2}+d_{m-1})} + \tfrac{1}{3}\,\frac{d_{m-1}\,d_m\,\mathbf{z}_m\,(d_{m+1}\mathbf{z}_m+d_m\mathbf{z}_{m+1})}{(d_{m-1}+d_m)(d_m+d_{m+1})}\\
&\quad + \textstyle\sum_{j=1}^{m-3} d_j\left(\tfrac{2}{3}\,\mathbf{z}_j^2 + \tfrac{1}{3}\,\frac{d_j\mathbf{z}_{j-1}+d_{j-1}\mathbf{z}_j}{d_{j-1}+d_j}\,\frac{d_{j+1}\mathbf{z}_j+d_j\mathbf{z}_{j+1}}{d_j+d_{j+1}}\right)\\
&\quad + \textstyle\sum_{j=1}^{m-2}(d_{j-1}+d_j)\,\frac{d_j\mathbf{z}_{j-1}+d_{j-1}\mathbf{z}_j}{d_{j-1}+d_j}\,(\mathbf{z}_{j-1}+\mathbf{z}_j).
\end{aligned}$$

Differently, if $m = 2$ conditions (30) are fulfilled by setting either

$$\mathbf{z}_1 = -\mathbf{z}_0\,\frac{3d_2^2+7d_2d_3+3d_3^2 \pm (d_2+d_3)\sqrt{-5(d_2^2+4d_2d_3+d_3^2)}}{7d_2^2+8d_2d_3+2d_3^2} \qquad \text{and} \qquad [\mathbf{z}_2,\mathbf{z}_3] = [\mathbf{z}_0,\mathbf{z}_1]$$

or

$$\mathbf{z}_1 = \pm\mathbf{z}_0\,\sqrt{-\frac{2d_2^3+10d_2^2d_3+15d_2d_3^2+5d_3^3}{5d_2^3+15d_2^2d_3+10d_2d_3^2+2d_3^3}} \qquad \text{and} \qquad [\mathbf{z}_2,\mathbf{z}_3] = -[\mathbf{z}_0,\mathbf{z}_1]. \tag{31}$$

We point out that, when $m = 2$, there are also two other solutions to (30), but we discard them because they provide values of $\mathbf{z}_1, \mathbf{z}_2, \mathbf{z}_3$ that imply $\mathbf{p}_6 = \mathbf{p}_7 = 0$ and thus, in light of (26), the resulting $\mathbf{r}$ would not be regular.

Since, in view of (26),

$$\mathbf{r}_{3m+2} = \mathbf{r}_2 + \sum_{j=2}^{3m+1}\frac{D_j}{5}\,\mathbf{p}_j, \quad \mathbf{r}_{3m+1} = \mathbf{r}_1 + \sum_{j=1}^{3m}\frac{D_j}{5}\,\mathbf{p}_j, \quad \mathbf{r}_{3m} = \mathbf{r}_0 + \sum_{j=0}^{3m-1}\frac{D_j}{5}\,\mathbf{p}_j,$$

we emphasize that conditions (30) imply

$$\mathbf{r}_{3m+2} = \mathbf{r}_2, \qquad \mathbf{r}_{3m+1} = \mathbf{r}_1 \qquad \text{and} \qquad \mathbf{r}_{3m} = \mathbf{r}_0. \tag{32}$$

Additionally, in view of (29) and (30), it also turns out that the last two and the first two control points of $\mathbf{p}$ satisfy

$$\mathbf{p}_{3m+1} = \mathbf{p}_1 \qquad \text{and} \qquad \mathbf{p}_{3m} = \mathbf{p}_0.$$

Moreover, when $m = 2$ and (31) holds, using (27) it is easy to prove that

$$\overline{\left(\frac{\mathbf{p}_0}{\mathbf{z}_0^2}\right)} = \frac{\mathbf{p}_4}{\mathbf{z}_0^2}, \qquad \overline{\left(\frac{\mathbf{p}_1}{\mathbf{z}_0^2}\right)} = \frac{\mathbf{p}_3}{\mathbf{z}_0^2} \qquad \text{and} \qquad \frac{\mathbf{p}_2}{\mathbf{z}_0^2}, \frac{\mathbf{p}_5}{\mathbf{z}_0^2} \in \mathbb{R}. \tag{33}$$

Thus, the control polygon $\{\mathbf{p}_0, \mathbf{p}_1, \mathbf{p}_2, \mathbf{p}_3, \mathbf{p}_4, \mathbf{p}_5\}$ is symmetric with respect to the line connecting $\mathbf{p}_2$ and $\mathbf{p}_5$. Similarly, using (26) and (29),

$$\begin{aligned}
\frac{\mathbf{r}_1-\mathbf{r}_0}{\mathbf{z}_0^2} &= \frac{d_1+d_2}{5}\,\frac{\mathbf{p}_0}{\mathbf{z}_0^2} = \frac{d_1+d_2}{5}\,\overline{\left(\frac{\mathbf{p}_4}{\mathbf{z}_0^2}\right)} = \overline{\left(\frac{\mathbf{r}_5-\mathbf{r}_4}{\mathbf{z}_0^2}\right)},\\
\frac{\mathbf{r}_2-\mathbf{r}_1}{\mathbf{z}_0^2} &= \frac{d_1+d_2}{5}\,\frac{\mathbf{p}_1}{\mathbf{z}_0^2} = \frac{d_1+d_2}{5}\,\overline{\left(\frac{\mathbf{p}_3}{\mathbf{z}_0^2}\right)} = \overline{\left(\frac{\mathbf{r}_4-\mathbf{r}_3}{\mathbf{z}_0^2}\right)},\\
\frac{\mathbf{r}_3-\mathbf{r}_2}{\mathbf{z}_0^2} &= \frac{d_1}{5}\,\frac{\mathbf{p}_2}{\mathbf{z}_0^2} \in \mathbb{R} \qquad \text{and} \qquad \frac{\mathbf{r}_0-\mathbf{r}_5}{\mathbf{z}_0^2} = \frac{\mathbf{r}_6-\mathbf{r}_5}{\mathbf{z}_0^2} = \frac{d_2}{5}\,\frac{\mathbf{p}_5}{\mathbf{z}_0^2} \in \mathbb{R}.
\end{aligned}$$

As a consequence, the control polygon $\{\mathbf{r}_0, \mathbf{r}_1, \mathbf{r}_2, \mathbf{r}_3, \mathbf{r}_4, \mathbf{r}_5\}$ is symmetric with respect to the line connecting $(\mathbf{r}_0+\mathbf{r}_5)/2$ and $(\mathbf{r}_2+\mathbf{r}_3)/2$.

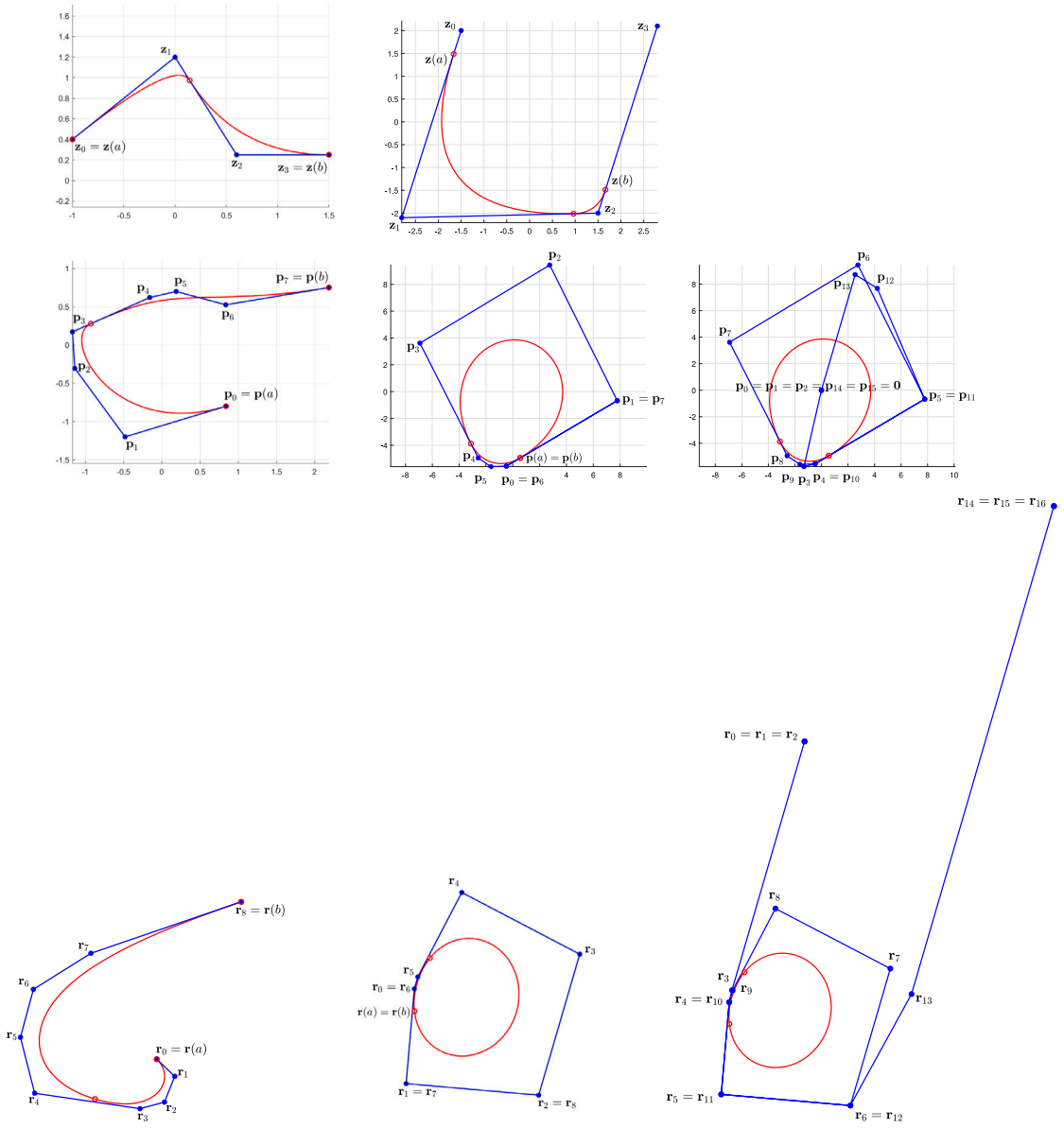

Fig. 4. Examples of quintic C^2 PH spline curves $\mathbf{r}(t)$ (third row), their quartic C^1 hodographs $\mathbf{p}(t)$ (second row) and their quadratic C^1 preimages $\mathbf{z}(t)$ (first row). First column: clamped case with $m = 2$. Second column: closed case with $m = 2$. Third column: representation of $\mathbf{p}$ and $\mathbf{r}$ used in [1] to get the same spline curves in the second column. In all figures red circles emphasize the junction points between consecutive polynomial pieces.

Remark 5. We conclude by pointing out that, in the closed case, the new definition of $\mathbf{r}$ and $\mathbf{p}$ is the one that guarantees the minimum possible number of knots. Indeed, recalling [1], the knot partition $\boldsymbol{\mu}$ would be $\{t_{-1} \le t_0 < a \equiv t_1 < t_2 < \cdots < t_m < t_{m+1} \equiv b < t_{m+2} \le t_{m+3}\}$ and, according to [15], the knot partition $\boldsymbol{\nu}$ associated to $\mathbf{p}(t) = \mathbf{z}^2(t)$ should be $\{\langle t_{-1}\rangle^3 \le \langle t_0\rangle^3 < \langle a \equiv t_1\rangle^3 < \langle t_2\rangle^3 < \cdots < \langle t_m\rangle^3 < \langle t_{m+1} \equiv b\rangle^3 < \langle t_{m+2}\rangle^3 \le \langle t_{m+3}\rangle^3\}$. But, in practice, the three-fold knot t_{-1} and the first of the t_0s could be erased since the quartic B-spline basis functions taking off from such knots would have a support that does not intersect the domain $[a, b]$ and hence would have no influence on the definition of $\mathbf{p}$. The same would happen for the quartic B-spline basis functions ending at the last of the t_{m+2}s and at each of the t_{m+3}s. As a consequence, differently from [1], Eq. (22) for a closed quintic PH B-spline with m polynomial pieces has eight fewer control points, i.e., $3m+3$ control points rather than $3m+11$ as suggested in [1] (see, e.g., Figs. 4 and 5 and compare (22) with [1, page 70]).

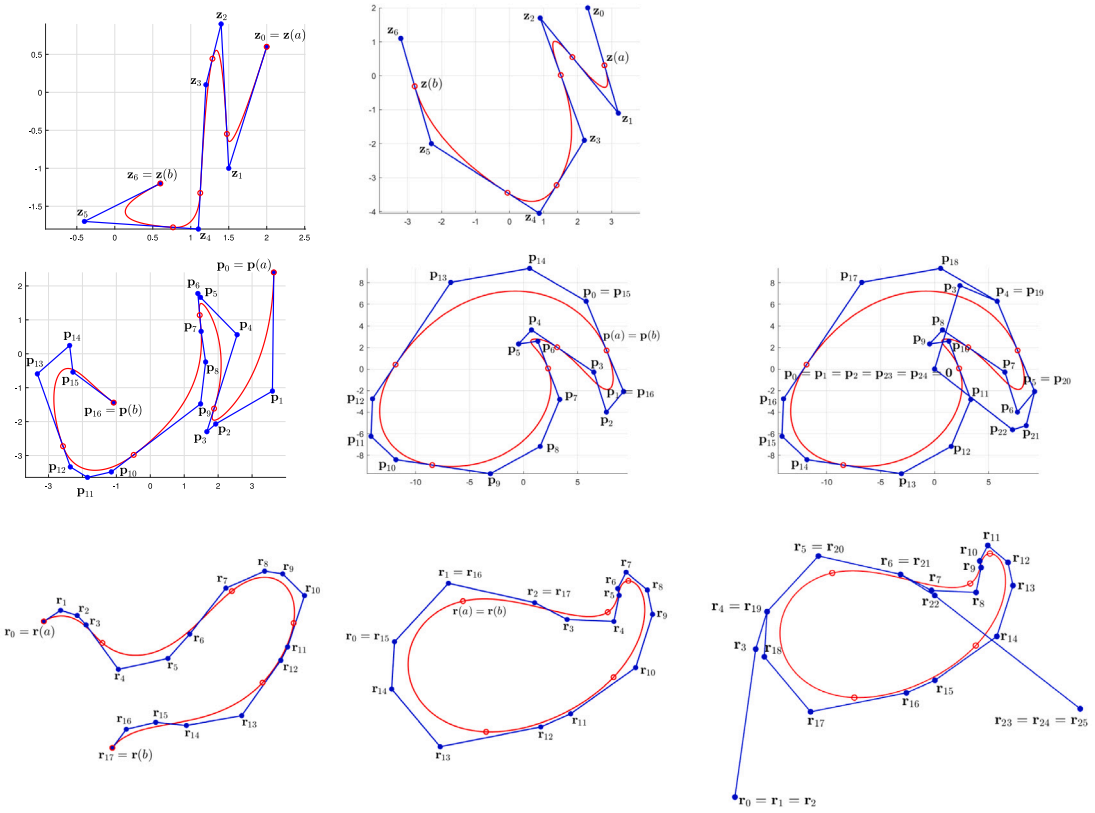

Fig. 5. Examples of quintic C^2 PH spline curves $\mathbf{r}(t)$ (third row), their quartic C^1 hodographs $\mathbf{p}(t)$ (second row) and their quadratic C^1 preimages $\mathbf{z}(t)$ (first row). First column: clamped case with $m = 5$. Second column: closed case with $m = 5$. Third column: representation of $\mathbf{p}$ and $\mathbf{r}$ used in [1] to get the same spline curves in the second column. In all figures red circles emphasize the junction points between consecutive polynomial pieces.

4.1. The unified complex algebraic characterization

For both the clamped and the closed cases the strategy to obtain the algebraic characterization of quintic PH B-splines is the following. First of all we observe that the quintic PH B-spline $\mathbf{r}(t)$ is defined for $t \in [a, b] = \cup_{j=1}^{m} [t_j, t_{j+1}]$ and is thus made of m polynomial pieces of degree 5 (see Fig. 6). Since $\mathbf{r}(t)$ is a polynomial curve on each interval $\mathcal{I}_j = [t_j, t_{j+1}]$, $j \in \{1, \dots, m\}$, it admits a representation in the Bernstein basis (or in Bézier form), i.e., for every $j \in \{1, \dots, m\}$, there exist $\{\mathbf{b}_{j,k} \in \mathbb{C}\}_{k=0}^{5}$ such that

$$\mathbf{r}\left((1-t)\,t_j + t\,t_{j+1}\right) \;=\; \sum_{k=0}^{5} \mathbf{b}_{j,k}\; B_k^5(t), \qquad \forall t \in [0,1],$$

where

$$B_k^5(t) \;=\; \binom{5}{k} (1-t)^{5-k}\, t^k.$$

Recalling the result in [16], later generalized in [17], the control points of the Bézier representation of each polynomial piece $\mathbf{r}(t)|_{t\in\mathcal{I}_j}$, $j \in \{1, \dots, m\}$, can be obtained from the control points $\mathbf{r}_{3(j-1)}, \dots, \mathbf{r}_{3(j-1)+5}$ of the spline representation by means of the B-spline-to-Bézier conversion matrix

$$S_j = \begin{bmatrix} \frac{(t_{j+1}-t_j)^2}{(t_{j+1}-t_{j-1})^2} & \frac{2(t_j-t_{j-1})(t_{j+1}-t_j)}{(t_{j+1}-t_{j-1})^2} & \frac{(t_j-t_{j-1})^2}{(t_{j+1}-t_{j-1})^2} & 0 & 0 & 0 \\ 0 & \frac{t_{j+1}-t_j}{t_{j+1}-t_{j-1}} & \frac{t_j-t_{j-1}}{t_{j+1}-t_{j-1}} & 0 & 0 & 0 \\ 0 & 0 & 1 & 0 & 0 & 0 \\ 0 & 0 & 0 & 1 & 0 & 0 \\ 0 & 0 & 0 & \frac{t_{j+2}-t_{j+1}}{t_{j+2}-t_j} & \frac{t_{j+1}-t_j}{t_{j+2}-t_j} & 0 \\ 0 & 0 & 0 & \frac{(t_{j+2}-t_{j+1})^2}{(t_{j+2}-t_j)^2} & \frac{2(t_{j+1}-t_j)(t_{j+2}-t_{j+1})}{(t_{j+2}-t_j)^2} & \frac{(t_{j+1}-t_j)^2}{(t_{j+2}-t_j)^2} \end{bmatrix},$$

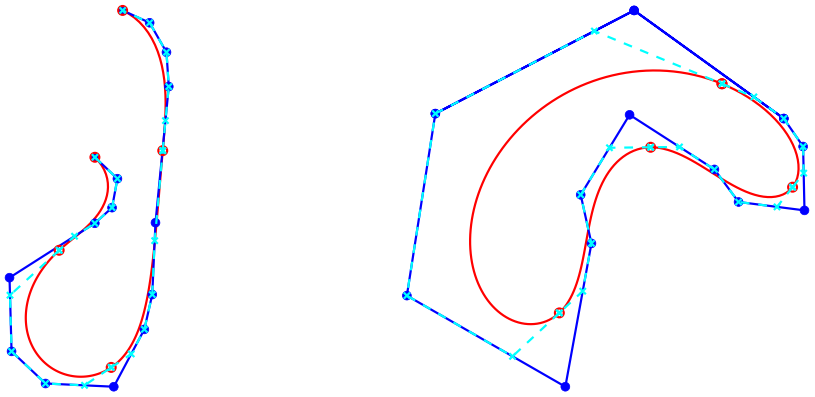

Fig. 6. Clamped (left) and closed (right) quintic PH B-spline curve with $m = 4$ and its m polynomial pieces. The jth curve piece ($j \in \{1, \dots, m\}$) is defined by the control points $\mathbf{r}_{3(j-1)}, \dots, \mathbf{r}_{3(j-1)+5}$.

which can be equivalently written in terms of d_{j-1}, d_j, d_{j+1} as

$$S_j = \begin{bmatrix} \frac{(d_j)^2}{(d_{j-1}+d_j)^2} & \frac{2d_{j-1}d_j}{(d_{j-1}+d_j)^2} & \frac{(d_{j-1})^2}{(d_{j-1}+d_j)^2} & 0 & 0 & 0 \\ 0 & \frac{d_j}{d_{j-1}+d_j} & \frac{d_{j-1}}{d_{j-1}+d_j} & 0 & 0 & 0 \\ 0 & 0 & 1 & 0 & 0 & 0 \\ 0 & 0 & 0 & 1 & 0 & 0 \\ 0 & 0 & 0 & \frac{d_{j+1}}{d_j+d_{j+1}} & \frac{d_j}{d_j+d_{j+1}} & 0 \\ 0 & 0 & 0 & \frac{(d_{j+1})^2}{(d_j+d_{j+1})^2} & \frac{2d_jd_{j+1}}{(d_j+d_{j+1})^2} & \frac{(d_j)^2}{(d_j+d_{j+1})^2} \end{bmatrix}. \tag{34}$$

Moreover, from [13], we know that $\mathbf{r}(t)|_{t\in\mathcal{I}_j}$ is a PH curve if and only if

$$\begin{cases} \mathbf{e}_{j,0}\,\mathbf{e}_{j,4} = \mathbf{k}_j^2, \\ \mathbf{e}_{j,0}\,\mathbf{e}_{j,4} = 3\,\mathbf{e}_{j,2}\,\mathbf{k}_j - 2\,\mathbf{e}_{j,1}\,\mathbf{e}_{j,3}, \end{cases} \tag{35}$$

where

$$\mathbf{e}_{j,k} \;=\; \mathbf{b}_{j,k+1} - \mathbf{b}_{j,k} \qquad \text{and} \qquad \mathbf{k}_j \;=\; 3\,\mathbf{e}_{j,2} - \left(\frac{\mathbf{e}_{j,1}^2}{\mathbf{e}_{j,0}} + \frac{\mathbf{e}_{j,3}^2}{\mathbf{e}_{j,4}}\right). \tag{36}$$

We then have the following three identities:

(i) due to (36),

$$\begin{bmatrix} \mathbf{e}_{j,0} \\ \mathbf{e}_{j,1} \\ \mathbf{e}_{j,2} \\ \mathbf{e}_{j,3} \\ \mathbf{e}_{j,4} \end{bmatrix} = \Delta \begin{bmatrix} \mathbf{b}_{j,0} \\ \mathbf{b}_{j,1} \\ \mathbf{b}_{j,2} \\ \mathbf{b}_{j,3} \\ \mathbf{b}_{j,4} \\ \mathbf{b}_{j,5} \end{bmatrix} \qquad \text{with} \qquad \Delta = \begin{bmatrix} -1 & 1 & 0 & 0 & 0 & 0 \\ 0 & -1 & 1 & 0 & 0 & 0 \\ 0 & 0 & -1 & 1 & 0 & 0 \\ 0 & 0 & 0 & -1 & 1 & 0 \\ 0 & 0 & 0 & 0 & -1 & 1 \end{bmatrix}; \tag{37}$$

(ii) due to (34),

$$\begin{bmatrix} \mathbf{b}_{j,0} \\ \mathbf{b}_{j,1} \\ \mathbf{b}_{j,2} \\ \mathbf{b}_{j,3} \\ \mathbf{b}_{j,4} \\ \mathbf{b}_{j,5} \end{bmatrix} = S_j \begin{bmatrix} \mathbf{r}_{3(j-1)} \\ \mathbf{r}_{3(j-1)+1} \\ \mathbf{r}_{3(j-1)+2} \\ \mathbf{r}_{3(j-1)+3} \\ \mathbf{r}_{3(j-1)+4} \\ \mathbf{r}_{3(j-1)+5} \end{bmatrix};$$

(iii) due to (26), where $\mathbf{r}_0$ is chosen to be 0 without loss of generality,

$$\begin{bmatrix} \mathbf{r}_0 \\ \vdots \\ \mathbf{r}_{3m+2} \end{bmatrix} = \frac{1}{5} \begin{bmatrix} 0 & & & & & & \\ d_0+d_1 & 0 & & & & & \\ d_0+d_1 & d_0+d_1 & 0 & & & & \\ \vdots & d_0+d_1 & d_1 & \ddots & & & \\ \vdots & \vdots & d_1 & \ddots & 0 & & \\ \vdots & \vdots & \vdots & \ddots & d_m & 0 & \\ \vdots & \vdots & \vdots & & d_m & d_m+d_{m+1} & 0 \\ d_0+d_1 & d_0+d_1 & d_1 & \cdots & d_m & d_m+d_{m+1} & d_m+d_{m+1} \end{bmatrix}_{(3m+3)\times(3m+2)} \begin{bmatrix} \mathbf{p}_0 \\ \vdots \\ \mathbf{p}_{3m+1} \end{bmatrix}.$$

Using the previous identities we can prove the following lemma.

Lemma 1. *For every $m \in \mathbb{N}$, $j \in \{1, \dots, m\}$,*

(a)

$$\Delta S_j \begin{bmatrix} 1 \\ 1 \\ 1 \\ 1 \\ 1 \\ 1 \end{bmatrix} = \begin{bmatrix} 0 \\ 0 \\ 0 \\ 0 \\ 0 \end{bmatrix};$$

(b)

$$\begin{bmatrix} \mathbf{e}_{j,0} \\ \mathbf{e}_{j,1} \\ \mathbf{e}_{j,2} \\ \mathbf{e}_{j,3} \\ \mathbf{e}_{j,4} \end{bmatrix} = \Delta S_j \, L_j \begin{bmatrix} \mathbf{p}_{3(j-1)} \\ \mathbf{p}_{3(j-1)+1} \\ \mathbf{p}_{3(j-1)+2} \\ \mathbf{p}_{3(j-1)+3} \\ \mathbf{p}_{3(j-1)+4} \end{bmatrix}$$

with

$$L_j = \frac{1}{5} \begin{bmatrix} 0 & 0 & 0 & 0 & 0 \\ d_{j-1}+d_j & 0 & 0 & 0 & 0 \\ d_{j-1}+d_j & d_{j-1}+d_j & 0 & 0 & 0 \\ d_{j-1}+d_j & d_{j-1}+d_j & d_j & 0 & 0 \\ d_{j-1}+d_j & d_{j-1}+d_j & d_j & d_j+d_{j+1} & 0 \\ d_{j-1}+d_j & d_{j-1}+d_j & d_j & d_j+d_{j+1} & d_j+d_{j+1} \end{bmatrix}.$$

In particular,

$$\begin{bmatrix} \mathbf{e}_{j,0} \\ \mathbf{e}_{j,1} \\ \mathbf{e}_{j,2} \\ \mathbf{e}_{j,3} \\ \mathbf{e}_{j,4} \end{bmatrix} = \frac{d_j}{5} \begin{bmatrix} \frac{d_j}{d_{j-1}+d_j} \mathbf{p}_{3(j-1)} + \frac{d_{j-1}}{d_{j-1}+d_j} \mathbf{p}_{3(j-1)+1} \\ \mathbf{p}_{3(j-1)+1} \\ \mathbf{p}_{3(j-1)+2} \\ \mathbf{p}_{3(j-1)+3} \\ \frac{d_{j+1}}{d_j+d_{j+1}} \mathbf{p}_{3(j-1)+3} + \frac{d_j}{d_j+d_{j+1}} \mathbf{p}_{3(j-1)+4} \end{bmatrix}. \tag{38}$$

Proof.

(a) Due to (34) and (37) we have

$$\Delta S_j = \begin{bmatrix} \frac{-(d_j)^2}{(d_{j-1}+d_j)^2} & \frac{d_j(d_j-d_{j-1})}{(d_{j-1}+d_j)^2} & \frac{d_{j-1}d_j}{(d_{j-1}+d_j)^2} & 0 & 0 & 0 \\ 0 & \frac{-d_j}{d_{j-1}+d_j} & \frac{d_j}{d_{j-1}+d_j} & 0 & 0 & 0 \\ 0 & 0 & -1 & 1 & 0 & 0 \\ 0 & 0 & 0 & \frac{-d_j}{d_j+d_{j+1}} & \frac{d_j}{d_j+d_{j+1}} & 0 \\ 0 & 0 & 0 & \frac{-d_j d_{j+1}}{(d_j+d_{j+1})^2} & \frac{d_j(d_{j+1}-d_j)}{(d_j+d_{j+1})^2} & \frac{(d_j)^2}{(d_j+d_{j+1})^2} \end{bmatrix}$$

from which the claim follows straightforwardly.

(b) Restricting (iii) to the rows having indices in $\{3(j-1),\dots,3(j-1)+5\}$ we have that

$$\begin{bmatrix} \mathbf{r}_{3(j-1)} \\ \mathbf{r}_{3(j-1)+1} \\ \mathbf{r}_{3(j-1)+2} \\ \mathbf{r}_{3(j-1)+3} \\ \mathbf{r}_{3(j-1)+4} \\ \mathbf{r}_{3(j-1)+5} \end{bmatrix} = \begin{bmatrix} R_j, & L_j, & \mathbf{0}_{6\times 3(m-j)} \end{bmatrix} \begin{bmatrix} \mathbf{p}_0 \\ \vdots \\ \mathbf{p}_{3m+1} \end{bmatrix},$$

where

$$R_j = \begin{bmatrix} 1 \\ 1 \\ 1 \\ 1 \\ 1 \\ 1 \end{bmatrix} \begin{bmatrix} d_0+d_1, & d_0+d_1, & d_1, & \dots, & d_{j-2}+d_{j-1}, & d_{j-2}+d_{j-1}, & d_{j-1} \end{bmatrix} \in \mathbb{R}^{6\times 3(j-1)}$$

is a rank-1 matrix. Thus,

$$\begin{bmatrix} \mathbf{r}_{3(j-1)} \\ \mathbf{r}_{3(j-1)+1} \\ \mathbf{r}_{3(j-1)+2} \\ \mathbf{r}_{3(j-1)+3} \\ \mathbf{r}_{3(j-1)+4} \\ \mathbf{r}_{3(j-1)+5} \end{bmatrix} = R_j \begin{bmatrix} \mathbf{p}_0 \\ \vdots \\ \mathbf{p}_{3(j-1)-1} \end{bmatrix} + L_j \begin{bmatrix} \mathbf{p}_{3(j-1)} \\ \mathbf{p}_{3(j-1)+1} \\ \mathbf{p}_{3(j-1)+2} \\ \mathbf{p}_{3(j-1)+3} \\ \mathbf{p}_{3(j-1)+4} \end{bmatrix},$$

and so, due to (i), (ii) and **(a)**,

$$\begin{bmatrix} \mathbf{e}_{j,0} \\ \mathbf{e}_{j,1} \\ \mathbf{e}_{j,2} \\ \mathbf{e}_{j,3} \\ \mathbf{e}_{j,4} \end{bmatrix} = \Delta\, S_j\, L_j \begin{bmatrix} \mathbf{p}_{3(j-1)} \\ \mathbf{p}_{3(j-1)+1} \\ \mathbf{p}_{3(j-1)+2} \\ \mathbf{p}_{3(j-1)+3} \\ \mathbf{p}_{3(j-1)+4} \end{bmatrix}.$$

In particular, it is easy to check that (38) holds true. □

Combining (35) and (38), we obtain the following result.

Theorem 1. *Let $m \in \mathbb{N}$ and $\mathbf{r}(t)$ be a regular planar quintic B-spline curve over the partition ρ in (21) with arbitrary control points $\{\mathbf{r}_i \in \mathbb{C}\}_{i=0}^{3m+2}$. Let, for every $j \in \{0,\dots,m\}$,*

$$\mathbf{w}_j = (1-w_j)\,\mathbf{p}_{3j} + w_j\,\mathbf{p}_{3j+1} \qquad \textit{with} \qquad w_j = \frac{d_j}{d_j+d_{j+1}}.$$

Then, $\mathbf{r}(t)$ is a PH B-spline if and only if, for every $j \in \{1,\dots,m\}$,

$$\begin{cases} \mathbf{w}_{j-1}\,\mathbf{w}_j = \mathbf{k}_j^2, \\ \mathbf{w}_{j-1}\,\mathbf{w}_j = 3\,\mathbf{p}_{3(j-1)+2}\,\mathbf{k}_j - 2\,\mathbf{p}_{3(j-1)+1}\,\mathbf{p}_{3(j-1)+3}, \end{cases} \tag{39}$$

where

$$\mathbf{k}_j = 3\,\mathbf{p}_{3(j-1)+2} - \left(\frac{\mathbf{p}_{3(j-1)+1}^2}{\mathbf{w}_{j-1}} + \frac{\mathbf{p}_{3(j-1)+3}^2}{\mathbf{w}_j} \right),$$

and $\{\mathbf{p}_i\}_{i=0}^{3m+1}$ are the control points of the hodograph of $\mathbf{r}(t)$ as specified in (23).

Remark 6. We observe that, for $j \in \{1,\dots,m-1\}$, $w_j \in]0,1[$, whereas $w_0 \in [0,1[$ and $w_m \in]0,1]$. Moreover, being $\mathbf{r}(t)$ regular, we have that

$$\mathbf{w}_{j-1} = \mathbf{r}'(t_j) \neq 0 \qquad \text{for all} \qquad j \in \{1,\dots,m+1\}. \tag{40}$$

Remark 7. For each $j \in \{1,\dots,m\}$, the quantity $\mathbf{k}_j d_j/5$ coincides with the *kern* (see [13, Definition 1]) of the quintic Bézier curve describing the jth polynomial piece of $\mathbf{r}(t)$.

Remark 8. In the clamped case, for $m=1$ we have $d_0 = d_2 = 0$ and thus (39) becomes

$$\begin{cases} \mathbf{p}_0\mathbf{p}_4 = \mathbf{k}_1^2, \\ \mathbf{p}_0\mathbf{p}_4 = 3\mathbf{p}_2\mathbf{k}_1 - 2\mathbf{p}_1\mathbf{p}_3, \end{cases}$$

where

$$\mathbf{k}_1 \;=\; 3\mathbf{p}_2 \;-\; \left(\frac{\mathbf{p}_1^2}{\mathbf{p}_0} \;+\; \frac{\mathbf{p}_3^2}{\mathbf{p}_4}\right),$$

which, as expected, gives us back the complex characterization of PH quintics found in [13, Corollary 2].

In the closed case, when $m = 2$ and (31) holds true, we have $d_0 = d_2$, $d_3 = d_1$ and, due to (33), we can observe that

$$\frac{\mathbf{w}_1\mathbf{w}_2}{\mathbf{z}_0^4} \;=\; \overline{\left(\frac{\mathbf{w}_0\mathbf{w}_1}{\mathbf{z}_0^4}\right)}, \qquad \frac{\mathbf{k}_2}{\mathbf{z}_0^2} \;=\; \overline{\left(\frac{\mathbf{k}_1}{\mathbf{z}_0^2}\right)} \qquad \text{and} \qquad \frac{3\mathbf{p}_5\mathbf{k}_2 \;-\; 2\mathbf{p}_4\mathbf{p}_6}{\mathbf{z}_0^4} \;=\; \overline{\left(\frac{3\mathbf{p}_2\mathbf{k}_1 \;-\; 2\mathbf{p}_1\mathbf{p}_3}{\mathbf{z}_0^4}\right)}.$$

As for the cubic case, the characterization given by conditions (39) allows us to verify if a given planar quintic B-spline is a PH B-spline using only the control points of the hodograph $\{\mathbf{p}_i\}_{i=0}^{3m+1}$. Conversely, given the control points of the hodograph satisfying (39), we are able to determine via (26) a regular planar quintic PH B-spline $\mathbf{r}(t)$ (unique up to a translation) and, of course, its parametric speed $|\mathbf{p}(t)|$. We conclude then proving that conditions (39) are enough also to fully identify the preimage $\mathbf{z}(t)$.

Proposition 2. *Let $\{\mathbf{p}_i \in \mathbb{C}\}_{i=0}^{3m+1}$ satisfy (39) and let $\mathbf{r}(t)$ be the regular planar quintic PH B-spline with hodograph control points $\{\mathbf{p}_i \in \mathbb{C}\}_{i=0}^{3m+1}$. Then, for $\mathbf{s}_0 \in \{\pm\sqrt{\mathbf{w}_0}\}$, the set of control points*

$$\begin{cases} \mathbf{z}_0 \;=\; \dfrac{\mathbf{p}_0}{\mathbf{s}_0}, \\ \mathbf{z}_1 \;=\; \dfrac{\mathbf{p}_1}{\mathbf{s}_0}, \\ \mathbf{z}_{j+1} \;=\; \dfrac{1}{w_j}\left(\dfrac{3\,\mathbf{p}_{3j-1} - 2\,\mathbf{z}_j^2}{(1-w_{j-1})\mathbf{z}_{j-1} + w_{j-1}\mathbf{z}_j} \;-\; (1-w_j)\,\mathbf{z}_j\right), \qquad j \in \{1,\dots,m\}. \end{cases} \tag{41}$$

defines a preimage of $\mathbf{r}(t)$.

Proof. First, defining $\{\mathbf{z}_j\}_{j=0}^{m+1}$ as in (41), we can obtain from the last m equations $\{\mathbf{p}_{3j-1}\}_{j=1}^{m}$ as

$$\mathbf{p}_{3j-1} \;=\; \frac{2}{3}\mathbf{z}_j^2 \;+\; \frac{1}{3}\big((1-w_{j-1})\mathbf{z}_{j-1} \;+\; w_{j-1}\mathbf{z}_j\big)\,\big((1-w_j)\mathbf{z}_j + w_j\mathbf{z}_{j+1}\big). \tag{42}$$

If (39) holds, then, for $j \in \{1,\dots,m\}$,

$$\begin{cases} \mathbf{w}_{j-1}\,\mathbf{w}_j \;=\; \left(3\mathbf{p}_{3j-1} - \left(\dfrac{\mathbf{p}_{3j-2}^2}{\mathbf{w}_{j-1}} + \dfrac{\mathbf{p}_{3j}^2}{\mathbf{w}_j}\right)\right)^2, \\ \mathbf{w}_{j-1}\,\mathbf{w}_j \;=\; 3\mathbf{p}_{3j-1}\left(3\mathbf{p}_{3j-1} - \left(\dfrac{\mathbf{p}_{3j-2}^2}{\mathbf{w}_{j-1}} + \dfrac{\mathbf{p}_{3j}^2}{\mathbf{w}_j}\right)\right) \;-\; 2\mathbf{p}_{3j-2}\mathbf{p}_{3j}. \end{cases}$$

Once $\mathbf{s}_0 \in \{\pm\sqrt{\mathbf{w}_0}\}$ is chosen, we can uniquely compute $\{\mathbf{s}_j \neq 0\}_{j=1}^{m}$ such that

$$\mathbf{s}_j^2 \;=\; \mathbf{w}_j,$$

and

$$\begin{cases} \mathbf{s}_{j-1}\,\mathbf{s}_j \;=\; 3\mathbf{p}_{3j-1} \;-\; \left(\dfrac{\mathbf{p}_{3j-2}}{\mathbf{s}_{j-1}}\right)^2 \;-\; \left(\dfrac{\mathbf{p}_{3j}}{\mathbf{s}_j}\right)^2, \\ \mathbf{s}_{j-1}^2\,\mathbf{s}_j^2 \;=\; 3\mathbf{p}_{3j-1}\left(3\mathbf{p}_{3j-1} \;-\; \left(\dfrac{\mathbf{p}_{3j-2}}{\mathbf{s}_{j-1}}\right)^2 \;-\; \left(\dfrac{\mathbf{p}_{3j}}{\mathbf{s}_j}\right)^2\right) \;-\; 2\mathbf{p}_{3j-2}\mathbf{p}_{3j}. \end{cases} \tag{43}$$

Plugging the first equation of (43) into the second one and then dividing by $\mathbf{s}_{j-1}\mathbf{s}_j$, we obtain

$$\mathbf{s}_{j-1}\,\mathbf{s}_j \;=\; 3\mathbf{p}_{3j-1} \;-\; 2\,\frac{\mathbf{p}_{3j-2}}{\mathbf{s}_{j-1}}\,\frac{\mathbf{p}_{3j}}{\mathbf{s}_j}.$$

But this, along with the first equation of (43), implies

$$\frac{\mathbf{p}_{3j-2}}{\mathbf{s}_{j-1}} \;=\; \frac{\mathbf{p}_{3j}}{\mathbf{s}_j},$$

and so the first equation of (43) can be simplified as

$$\mathbf{s}_{j-1}\,\mathbf{s}_j \;=\; 3\mathbf{p}_{3j-1} \;-\; 2\left(\frac{\mathbf{p}_{3j-2}}{\mathbf{s}_{j-1}}\right)^2 \;=\; 3\mathbf{p}_{3j-1} \;-\; 2\left(\frac{\mathbf{p}_{3j}}{\mathbf{s}_j}\right)^2. \tag{44}$$

Observing that, according to the first two equations in (41),

$$(1-w_0)\mathbf{z}_0 \;+\; w_0\mathbf{z}_1 \;=\; \frac{(1-w_0)\,\mathbf{p}_0 \;+\; w_0\mathbf{p}_1}{\mathbf{s}_0} \;=\; \frac{\mathbf{w}_0}{\mathbf{s}_0} \;=\; \mathbf{s}_0,$$

then, combining (42) and (44) for $j = 1$, we get

$$\mathbf{s}_1 \;=\; (1-w_1)\mathbf{z}_1 \;+\; w_1\mathbf{z}_2 \qquad \text{and} \qquad \mathbf{p}_3 \;=\; \mathbf{z}_1\,\mathbf{s}_1.$$

In a similar way, one can prove that, for every $j \in \{1, \dots, m\}$,

$$\mathbf{s}_j = (1-w_j)\,\mathbf{z}_j + w_j \mathbf{z}_{j+1}, \quad \text{and} \quad \mathbf{p}'_{3j} = \mathbf{z}_j\,\mathbf{s}_j \qquad \mathbf{p}_{3j+1} = \mathbf{z}_{j+1}\,\mathbf{s}_j. \tag{45}$$

But (42) and (45) coincide with conditions (27) and so $\mathbf{r}'(t) = \mathbf{z}^2(t)$. □

Remark 9. As in the cubic case, the preimage of $\mathbf{r}(t)$ is identified up to a sign, given by the choice of $\mathbf{s}_0$. With respect to the known result (see Eq. (41) and Eq. (43) in [1]), here (41) is without ambiguities about the signs of $\{\mathbf{z}_j\}_{j=0}^{m+1}$. This is a benefit brought by Theorem 1.

5. Conclusion and future work

In this work we focused our attention on low degree PH B-spline curves. In particular, we presented a simplified and unified representation of clamped and closed planar PH B-spline curves of degree three and five, providing conditions on their preimage in order to have closed ones. The presented results are easily extendable to planar PH B-spline curves of any odd degree. Moreover, we introduced a *complex* algebraic characterization for such curves that, on one side, generalizes the one already known for PH cubics [11,12] and quintics [13] and, on the other side, allows users to easily establish whether a given C^1 cubic / C^2 quintic spline curve has the PH property or not. Additionally, we have exploited the proposed algebraic characterization to fully identify the preimage of a regular planar cubic/quintic PH B-spline curve resolving the sign ambiguities that affected the results in [1]. In our future work we plan to derive a geometric interpretation of our algebraic conditions and to propose applications exploiting them to construct C^2 quintic PH B-spline curves.

Acknowledgments

This research has been accomplished within RITA (Research ITalian network on Approximation) and UMI-TAA. The authors are members of the INdAM research group GNCS (Gruppo Nazionale Calcolo Scientifico - Istituto Nazionale di Alta Matematica). The work was partially supported by the "INdAM - GNCS Research Project" identified by the code CUP_E53C23001670001.

The authors are grateful to the reviewers for the time spent to review this manuscript and for their valuable suggestions.

Data availability

No data was used for the research described in the article.

References

[1] G. Albrecht, C.V. Beccari, J.-C. Canonne, L. Romani, Planar Pythagorean-Hodograph B-spline curves, Comput. Aided Geom. Design 57 (2017) 57–77.
[2] G. Albrecht, C.V. Beccari, L. Romani, Spatial Pythagorean-Hodograph B–spline curves and 3D point data interpolation, Comput. Aided Geom. Design 80 (2020) 101868.
[3] G. Albrecht, C.V. Beccari, L. Romani, G^2/C^1 Hermite interpolation by planar PH B-spline curves with shape parameter, Appl. Math. Lett. 121 (2021) 107452.
[4] G. Albrecht, C.V. Beccari, L. Romani, Interpolating sequences of 3D-data with C^2 quintic PH B-spline curves, Dolomites Res. Notes Approx. 15 (3) (2022) 1–11.
[5] M. Bizzarri, M. Lávička, Interpolation of Hermite data by clamped Minkowski Pythagorean Hodograph B-spline curves, J. Comput. Appl. Math. 392 (2021) 113469.
[6] M. Bizzarri, M. Lávička, J. Vršek, C^d Hermite interpolations with spatial Pythagorean Hodograph B-splines, Comput. Aided Geom. Design 87 (2021) 101992.
[7] M. Bizzarri, M. Lávička, Construction of Minkowski Pythagorean Hodograph B-spline curves, Comput. Aided Geom. Design 80 (2020) 101878.
[8] M. Bizzarri, K. Kadlec, M. Lávička, Z. Šír, B-spline Pythagorean Hodograph curves in clifford algebras, Adv. Appl. Clifford Algebr. 33 (1) (2023) 9.
[9] R.T. Farouki, C. Giannelli, A. Sestini, Local modification of Pythagorean-hodograph quintic spline curves using the B-spline form, Adv. Comput. Math. 42 (2016) 199–225.
[10] R.T. Farouki, C. Giannelli, A. Sestini, Identification and reverse engineering of Pythagorean-hodograph curves, Comput. Aided Geom. Design 34 (2015) 21–36.
[11] R.T. Farouki, The conformal map $z \to z^2$ of the hodograph plane, Comput. Aided Geom. Design 11 (1994) 363–390.
[12] R.T. Farouki, Pythagorean-Hodograph Curves: Algebra and Geometry Inseparable. Geometry and Computing, 1, Springer, Berlin, 2008.
[13] K. Hormann, L. Romani, A. Viscardi, New algebraic and geometric characterizations of planar quintic Pythagorean-hodograph curves, Comput. Aided Geom. Design 108 (2024) 102256.
[14] K. Mørken, Some identities for products and degree raising of splines, Constr. Approx. 7 (1991) 195–208.
[15] A.H. Vermeulen, R.H. Bartels, C.R. Heppler, Integrating products of B-splines, SIAM J. Sci. Stat. Comput. 13 (4) (1992) 1025–1038.
[16] L. Romani, M.A. Sabin, The conversion matrix between uniform B-spline and Bézier representations, Comput. Aided Geom. Design 21 (2004) 549–560.
[17] G. Casciola, L. Romani, A general matrix representation for non-uniform B-spline subdivision with boundary control, in: ALMA-DL, 2532, Digital Library of the University of Bologna, 2007, pp. 1–12, AMS Acta c.i. Available at http://amsacta.cib.unibo.it/archive/00002532.